14th European Signal Processing Conference (EUSIPCO 2006), Florence, Italy, September 4-8, 2006, copyright by EURASIP

BAYESIAN INFERENCE FOR MULTIDIMENSIONAL NMR IMAGE RECONSTRUCTION

[1]*Ji Won Yoon, and* [2]*Simon J. Godsill*

Signal Processing Group, Cambridge University
Trumpington Street, CB2 1PZ, Cambridge, U.K.
[1]phone: + (44) 7771-964-170, fax: + (44) 1223 332662, email: jwy20@cam.ac.uk
web: http://www-sigproc.eng.cam.ac.uk/∼jwy20
[2]phone: + (44) 1223-332-604, fax: + (44) 1223 332662, email: sjg@eng.cam.ac.uk
web: http://www-sigproc.eng.cam.ac.uk/∼sjg

ABSTRACT

Reconstruction of an image from a set of projections has been adapted to generate multidimensional nuclear magnetic resonance (NMR) spectra, which have discrete features that are relatively sparsely distributed in space. For this reason, a reliable reconstruction can be made from a small number of projections. This new concept is called Projection Reconstruction NMR (PR-NMR). In this paper, multidimensional NMR spectra are reconstructed by Reversible Jump Markov Chain Monte Carlo (RJMCMC). This statistical method generates samples under the assumption that each peak consists of a small number of parameters: position of peak centres, peak amplitude, and peak width. In order to find the number of peaks and shape, RJMCMC has several moves: birth, death, merge, split, and invariant updating. The reconstruction schemes are tested on a set of six projections derived from the three-dimensional 700 MHz HNCO spectrum of a protein HasA.

1. INTRODUCTION

Multidimensional NMR spectroscopy is well known to be very useful for protein structure determination. However, it has a serious drawback, speed. The minimum measurement time of an N-dimensional NMR experiment increases as the number of dimensions increases. This makes multidimensional NMR spectroscopy intractable in practice. For these reasons, several investigators have been trying to speed up these measurements by more efficient approaches. Many approaches based on the demands are traced back to the concept of *accordion spectroscopy*[1]. GFT-NMR [2] and Projection Reconstruction NMR (PR-NMR) [3, 4, 5, 6, 7] address this problem. PR-NMR considered in this paper speeds up the acquisition of multidimensional NMR spectra by reconstructing them from a small number of projections. The procedure is related to that used in X-ray, computed tomography (CT) and fMRI which have been approached by several statistical methods such as maximum likelihood [8], EM algorithm [9], maximum entropy [10, 11, 12] and maximum a posteriori using Gibbs prior [13]. We have applied several of these methods to PR-NMR [14]. However, these methods are best suited to CT and X-ray tomography where the physiological object is continuous, in contrast to the discrete peak property of an NMR spectrum. Therefore, we propose RJMCMC to reconstruct the discrete NMR spectra. RJMCMC searches for the number and the shape of discrete peaks under the assumption that each discrete peak consists of a small number of parameters: centre position, amplitude, and line-width.

This paper mainly consists of three sections. In the first section, we define the models for multidimensional NMR. The next section demonstrates the design of Bayesian models for the PR-NMR. RJMCMC algorithms are explained in this section as well. In the last section, RJMCMC reconstruction is compared with Maximum Entropy reconstruction with an experimental data with 6 projections.

2. MODELS FOR MULTIDIMENSIONAL NMR

Reconstruction of multidimensional NMR spectra from a small number of projections can be achieved by two strategies: pixel-by-pixel modeling and peak-by-peak modeling. While pixel-by-pixel modeling determines all pixels on an image individually in terms of the given projections, the peak-by-peak approach reconstructs an image using a finite collection of specific peak shapes. Even though the peak-by-peak model is an idealisation of reality, it is a very reasonable assumption, in that the NMR peak shape can be well approximated as a specific shape such as Gaussian or Lorentzian. In the peak-by-peak approach, each peak consists of centre position, amplitude, and peak-width. Peak-by-peak estimation can be more efficient since it models explicitly the sparseness inherent in the NMR spectra. Thus, in the peak-by-peak approach, we do not have to directly update all areas of the image as would be done in the pixel-by-pixel approach. Another interpretation is that a solution can rapidly be obtained since the number of parameters for peak-by-peak estimation is much smaller than that for pixel-by-pixel. Here, then, we define the underlying image model at pixel location x with a finite collection of peaks,

$$S(x) = \sum_{k=1}^{K} A_k \phi(x|\mu_k, \Sigma) \tag{1}$$

$$\phi(x|\mu_k,\Sigma) = \frac{1}{\sqrt{\det(2\pi\Sigma)}} \exp\left\{ -\frac{1}{2}(x-\mu_k)^T \Sigma^{-1}(x-\mu_k) \right\}$$

where $S(x)$ is the intensity at the image position x and

$$\begin{aligned} x &= [x_1, x_2]^T \\ \mu_k &= [\mu_{k,1}, \mu_{k,2}]^T \\ \Sigma &= \sigma^2 I \end{aligned}$$

In Eq. (1), A_k is the amplitude of kth peak. The radial function ϕ denotes the specific peak shape such as Gaussian, Lorentzian, or Laplacian shape. In this paper, we use the Gaussian shape for the radial functions ϕ, which has two components: μ_k for centre position and σ for peak-width. In NMR spectroscopy, the width of the peaks are considered almost constant. Thus, we use a single width parameter σ in order to reduce the total number of parameters, and this speeds up RJMCMC. However, in earlier work we also experimented successfully with variable peak widths within each image.

In PR-NMR, input data are a small number of projections obtained at different projection angles. Suppose that Y is the projection data. λ_i and s stand for the ith projection angle and the sample index into a projection, respectively, $i = 1, \cdots, \vartheta$. φ_i denotes a scaling factor, which varies with the projection number, i. The PR-NMR data is then defined as

$$Y_s^i = \varphi_i R(S, \lambda_i, s) + \varepsilon_{\lambda_i} \tag{2}$$

where Y_s^i is the sth data-point of ith projection taken at angle λ_i and $R(S,\lambda_i,s)$ is the projection function for the ith angle λ_i and data point as follows:

$$R(S,\lambda_i,s)=\int_{-\infty}^{\infty}\int_{-\infty}^{\infty}S(x)\delta(x_1\cos\lambda_i+x_2\sin\lambda_i-s)dx_1dx_2 \quad (3)$$

Suppose that the number of data points in each projection is M and the number of peaks is K. Eq. (2) can be written in the linear model framework using vector notation as follows:

$$Y=XA_{1:K}+e \text{ where } e\overset{iid}{\sim}N(e;0,\sigma_e^2I) \quad (4)$$

where σ_e is assumed known. Y is the stacked vector of projection data, defined as follows:

$$Y^T=\left[Y_1^1,\cdots,Y_M^1,\cdots,Y_1^\vartheta,\cdots,Y_M^\vartheta\right] \quad (5)$$

X denotes the integrated peaks obtained by substituting Eq. (1) into Eq. (3) in terms of angles λ and scaling factors φ and $A_{1:K}=[A_1,A_2,\cdots,A_K]$ is a vector of peak amplitudes. e is a noise vector. When we have ϑ projections, X is a matrix with size $(M\vartheta)\times K$ and $A_{1:K}$ is a $K\times 1$ vector. The size of Y and e vectors is $(M\vartheta)$. For instance, when we have $\vartheta=4$ projections with $M=100$ points and the image has 3 peaks, the size of matrices Y, X, and $A_{1:K}$ are 400×1, 400×3, and 3×1 respectively.

3. BAYESIAN MODELS FOR PR-NMR

The peak-by-peak approach presents a computational challenge in that the number of peaks are not known apriori. In order to estimate the number of peaks, trans-dimensional methods can be applied. One of the most useful trans-dimensional approaches is Reversible Jump Markov Chain Monte Carlo (RJMCMC) [15, 16, 18, 19], a promising approach that we adapt for finding peaks in multidimensional NMR spectroscopy.

Denote by $\theta_k\in\Theta_k$ the parameter vector associated with the peak indexed by $k\in\kappa$, then for K peaks we have the model:

$$\begin{aligned}\theta_{1:K} &= (\mu_{1:K},A_{1:K},\sigma,\varphi_{1:\vartheta}) \text{ where } \mu_{1:K}=(\mu_{1,1:K},\mu_{2,1:K}) \quad (6)\\ A_k &\overset{iid}{\sim} N(A_k;\mu_A,C_A)\\ \mu_{k,1} &\overset{iid}{\sim} U(\mu_{k,1};0,T_1)\\ \mu_{k,2} &\overset{iid}{\sim} U(\mu_{k,2};0,T_2)\\ \sigma &\overset{iid}{\sim} G(\sigma-t|\alpha,\beta)\\ \varphi_i &\overset{iid}{\sim} U(\varphi_i;0,1)\end{aligned}$$

where $k\in\{1,\cdots,k_{max}\}$ and $K\le k_{max}$. α,β,μ_A,C_A and $t>0$ are assumed known. T_1 and T_2 are the dimensions of the image which we reconstruct. N, U, and G denote normal, uniform, and Gaussian distribution respectively. Since the trans-dimensional MCMC is a generalisation of fixed dimensional MCMC, the overall parameter space for θ can be written as a countable union of subspaces having different dimensionality, [15]

Owing to the linear Gaussian assumption for A and the likelihood, we can remove $A_{1:K}$ by analytical integration,

$$\begin{aligned}P(\mu_{1:K},\sigma,\varphi_{1:\vartheta}|Y) &= \int P(\mu_{1:K},A_{1:K},\sigma,\varphi_{1:\vartheta}|Y)dA_{1:K}\\ &= \int P(Y,A_{1:K}|\mu_{1:K},\sigma,\varphi_{1:\vartheta})dA_{1:K}P(\mu_{1:K},\sigma,\varphi_{1:\vartheta})\\ &= P(Y|\mu_{1:K},\sigma,\varphi_{1:\vartheta})P(\mu_{1:K},\sigma,\varphi_{1:\vartheta}) \quad (7)\end{aligned}$$

The removal of the nuisance parameters makes RJMCMC more efficient (Rao-Blackwellization). Note that although $A_{1:K}$ is marginalised, we sequently require estimates of $A_{1:K}$ and these can be obtained from the full conditional $P(A_{1:K}|\mu_{1:K},\varphi_{1:\vartheta},\sigma,Y)$, where required for estimation as in [17, 18]. The likelihood $P(Y|\mu_{1:K},\sigma,\varphi_{1:\vartheta})$ is defined by

$$\begin{aligned}P(Y|\mu_{1:K},\sigma,\varphi_{1:\vartheta}) &= \frac{1}{(2\pi)^N|C_A|^{1/2}|\Phi|^{1/2}(\sigma_e^2)^{(N-N_A)/2}}\\ &\times\exp\left\{-\frac{1}{2\sigma_e^2}(Y^TY+\sigma_e^2\mu_A^TC_A^{-1}\mu_A-\phi^T\hat{A})\right\} \quad (8)\end{aligned}$$

$$\begin{aligned}\text{where } \hat{A} &= \Phi^{-1}\phi\\ \Phi &= X^TX+\sigma_e^2C_A^{-1}\\ \phi &= X^TY+\sigma_e^2C_A^{-1}\mu_A\end{aligned}$$

Here, N and N_A are the number of elements in the vectors Y and $A_{1:K}$ respectively.

3.1 Main procedure for RJMCMC

The RJMCMC for PR-NMR has the following procedure in this paper:

- Propose a type of move from Birth, Death, Split, Merge, and Dimension invariant.
- If the move type is Dimension invariant, RJMCMC samples parameters using a standard Metropolis-Hastings (MH) algorithm, so that each unknown parameter is updated according to an acceptance probability

$$\alpha_K=\min\left\{1,\frac{P(y|\theta'_{1:K})P(\theta'_{1:K})q(\theta_{1:K};\theta'_{1:K})}{P(y|\theta_{1:K})P(\theta_{1:K})q(\theta'_{1:K};\theta_{1:K})}\right\} \quad (9)$$

- If the move type is one of Birth, Death, Split, and Merge, RJMCMC follows a generalized MH step with acceptance probabilities

$$\alpha_{K'}=\min\left\{1,\frac{P(y|K',\theta'_{1:K'})P(K')P(\theta'_{1:K'}|K')q_1(K;K')q_2(\theta_{1:K};\theta'_{1:K'})}{P(y|K,\theta_{1:K})P(K)P(\theta_{1:K}|K)q_1(K';K)q_2(\theta'_{1:K'};\theta_{1:K})}\right\} \quad (10)$$

Note that we do not require Green's Jacobian terms in our algorithm as in [18]. Note here that θ and θ' are interpreted as $\mu_{1:K},\sigma$, i.e. Note also that the scaling factors $\varphi_{1:\vartheta}$ are sampled using standard Gibbs step, not detailed here.

3.2 Dimension invariant moves

The RJMCMC is the same as MCMC in case of Dimension invariant in that the dimension is fixed as in Eq. (9). For the Dimension invariant, internal terms are designed for fixed dimensional MCMC. In the Eq. (9), $\theta_{1:K}$ has two different types of parameters, $\mu_{1:K}$ and σ. We estimate the parameters separately. That is, Dimension invariant move has two steps: one for position estimation and the other for the peak width. The prior structure of $\theta_{1:K}$ is assumed to be

$$P(\theta_{1:K})=P(\sigma)\prod_{k=1}^{K}P(\mu_k)P(A_k) \quad (11)$$

In order to make a simple but reasonable kernel function, $q(\theta'_{1:K'};\theta_{1:K})$, the parameters are proposed as follows:

$$\theta'_{1:K}\sim q(\theta'_{1:K}|\theta_{1:K}) = \begin{cases}G(\sigma'-t|\alpha,\beta)\\ N(\mu'_{i,1}|\mu_{i,1},\varsigma^2)\times N(\mu'_{i,2}|\mu_{i,2},\varsigma^2)\end{cases}$$

where ς is assumed known.

3.3 Other moves : Birth, Death, Split, and Merge moves

3.3.1 Prior distributions for K and $\theta_{1:K}|K$

The several moves in Eq. (10) have more complicated equations. $P(K)$ is a prior distribution for dimensionality and we use a uniform distribution for the random variable K. $P(\theta_{1:K}|K)$ is a prior distribution for the parameters. However, unlike the dimension invariant move, we only estimate the positions $\mu_{1:K}$ with the fixed width σ to increase the acceptance ratios. Specific prior knowledge may be applicable to $P(\mu_k|K)$ but in this paper we have assumed a uniform distribution for $P(\mu_k|K)$.

3.3.2 A transition kernel for the dimension

$q_1(K^{'}|K)$ proposes the new number of peaks. We apply several moves such as Birth, Death, Split and Merge moves. All moves have only one difference between the current step and the proposed step. That is, the Birth and Split moves increase the number of peaks by one and Death and Merge moves decrease it by one. Therefore, the probability for $q_1(K^{'}|K)$ is defined as

$$q_1(K^{'}|K) = \begin{cases} 1 & \text{for Birth} \\ \frac{1}{K} & \text{for Death, Split and Merge} \end{cases} \tag{12}$$

3.3.3 A transition kernel for parameters : Birth and Death moves

$q_2(\theta^{'}_{1:K^{'}}|\theta_{1:K})$ consists of two elements, $\mu_{k,1}$ and $\mu_{k,2}$ for the centre position of the kth peak respectively. In Birth and Death moves, the transition kernel function is a random map. Thus the transition probability is defined the same as the prior distribution of the parameters. Therefore, this term in the RJMCMC is canceled out. When $P(K)$ and $P(K^{'})$ follow a uniform distribution, Eq. (10) is defined as

$$\begin{aligned} \alpha_{K^{'}} &= \min\left\{1, \frac{P(y|K^{'},\theta^{'}_{1:K^{'}})q_1(K;K^{'})}{P(y|K,\theta_{1:K})q_1(K^{'};K)}\right\} \\ &\text{where } \theta^{'}_{1:K^{'}} \sim q_2(\theta^{'}_{1:K^{'}};\theta_{1:K}) = P(\theta^{'}_{1:K^{'}}|K^{'}) \end{aligned} \tag{13}$$

3.3.4 A transition kernel for parameters : Split and Merge moves

Since Split and Merge moves may work with specific geometric maps rather than random maps, their transition kernels may be different from the Birth and Death moves. For example, if μ_i is selected to be split, $\mu_i^{'}$ may be chosen by $N(\mu_i^{'};\mu_i,\omega^2)$ where ω is the specific range for Split. Both moves depend upon the previous parameters and the probabilities of the Split and Merge moves in a peak are designed by

$$\begin{aligned} \mu^{'}_m &\sim q_2(\mu^{'}_m|\mu_k) = N(\mu^{'}_m;\mu_k,\lambda) \text{ for Split} \\ \mu^{'}_n &\sim q_2(\mu^{'}_n|\mu_k) = N(\mu^{'}_n;\mu_k,\lambda) \text{ for Split} \\ \mu^{'}_k &\sim q_2(\mu^{'}_k|\mu_m,\mu_n) = N(\mu^{'}_k;\bar{\mu},\upsilon) \text{ for Merge} \\ &\begin{cases} \bar{\mu} = \mu_m \times \omega_m + \mu_n \times \omega_n \\ \omega_m = \frac{A_m}{A_m+A_n} \\ \omega_n = \frac{A_n}{A_m+A_n} \end{cases} \end{aligned} \tag{14}$$

where λ and υ are assumed known.

3.4 Estimating amplitudes, $A_{1:K}$

Finally, we sample amplitude parameters from

$$A_{1:K} \sim P(A_{1:K}|Y,C_A,\mu_A,\sigma_e^2) = N(\hat{A},\sigma_e^2\Phi^{-1}) \tag{15}$$

4. RESULTS

4.1 Experimental data

Fig. (1) shows the experimental data set for reconstruction of NMR spectra using RJMCMC. They are projections of $^{13}C^{15}N$ correlation peaks in the 700MHz HNCO spectrum of the protein *HasA*. The projection angles are determined by the ratio of the evolution increments $\Delta t_2/\Delta t_1$. Only 6 projections with angles $+30^0$, -30^0, $+50^0$, -50^0, 0^0 and $+90^0$ are used to reconstruct NMR spectra having 16 peaks.

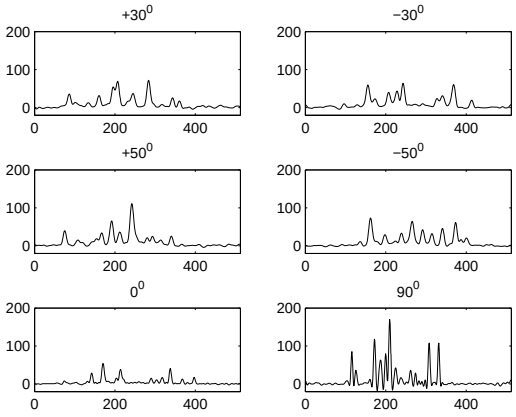

Figure 1: Experimental NMR Projections

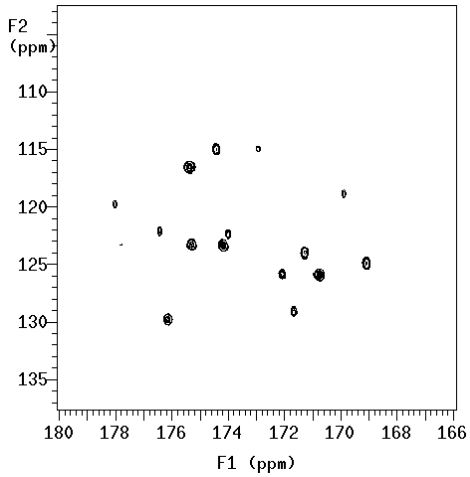

Figure 2: A contour of an experimental target map

Fig. (2) shows the contour image of a desired target map. The F_1F_2 plane extracted from the full three-dimensional HNCO experiment on *HasA*, performed by the conventional method where both evolution times are incremented independently. The 16 peaks include a doublet and very weak peaks as in Fig. (2).

4.2 Convergence

RJMCMC runs 40,000 iterations including 20,000 sampling and 20,000 burn-in periods. The initial state is randomly selected with a random number of peaks. All moves are retrieved in each iteration - Birth, Death, Split, Merge and Dimension invariant for $\mu_{1:K}$ and σ. Fig. (3) shows the trajectory of the number of peaks (top) and the probability density $P(K|y)$ of the number of peaks (bottom) for the simulation. We can see that RJMCMC arrives at a stationary state around $K = 20$. Fig. (4) shows the trajectory of the peak width (top) and its probability density function $P(\sigma|y)$ (bottom). To plot the $P(K|y)$ and $P(\sigma|y)$, we use *ksdensity* in Matlab with $npoints = 100$ and $width = 1$. As in both figures, the number of peaks, K and the peak-width, σ follow an almost normal distribution with mean 20 and 2.9 respectively.

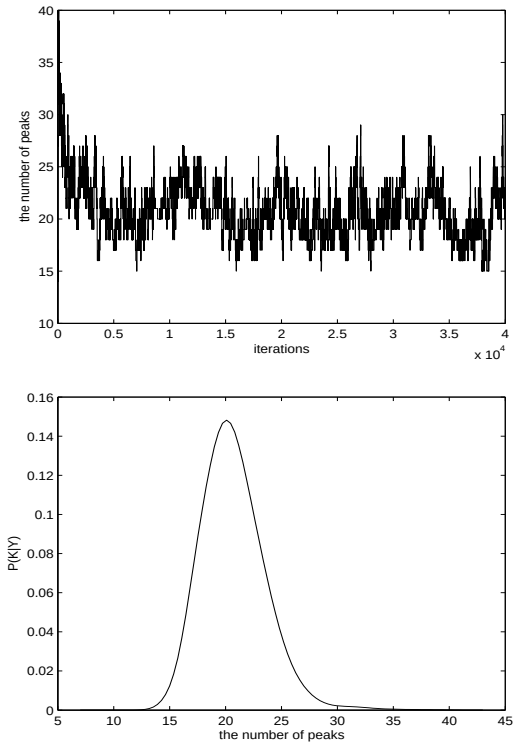

Figure 3: The number of peaks of an image from RJMCMC

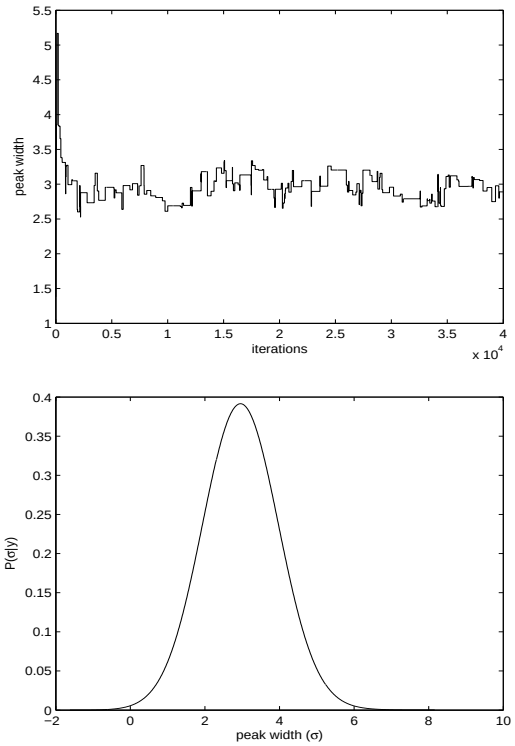

Figure 4: Peak-width from RJMCMC

4.3 Comparison

We compare the results of RJMCMC with that of maximum entropy [12] which is a well-known method in reconstruction. Fig. (5) and (6) show that the reconstructed image from maximum entropy has serious problems with the poor detection of peaks and the incorrect intensities of detected peaks. In comparison, RJMCMC detects almost all peaks including very small peaks as in Fig. (7) and (8). In addition, although Monte Carlo methods are known to be slow, RJMCMC reconstruction may be faster than maximum entropy reconstruction which is based on pixel-by-pixel estimation, since the RJMCMC reconstruction estimates a far smaller number of parameters. However, a weak peak and a doublet are not detected in Fig. (7). The peaks are located at $(174, 122)$, and $(177.8, 123.1)$ in Fig. (2). The weakest peak at $(177.8, 123.1)$ is also detected but a few artifacts appear as the contour levels decrease. However, we cannot find the doublet at $(174, 122)$ in very low contour levels. Even though RJMCMC does not detect a few weak peaks, it gives much better results than any other approaches including Maximum Entropy. In time comparison, RJMCMC reconstruction takes 80 minutes while Maximum Entropy reconstruction takes 30 minutes with this experimental data on a computer with the processor speed of 1.73GHz.

5. CONCLUSION

With a small number of projections, Projection Reconstruction NMR (PR-NMR) can reconstruct multi-dimensional NMR spectra efficiently. In this paper, Reversible Jump Markov Chain Monte Carlo (RJMCMC) is applied to reconstruct discrete NMR spectra from a small number of projections. RJMCMC searches for the number of peaks and widths, positions, and amplitudes of the peaks automatically. RJMCMC reconstruction gives a much better image than Maximum Entropy reconstruction. Also, it is known that NMR suffers from noise and Maximum Entropy reconstruction does not work well for a noisy image. However, RJMCMC reconstruction is very robust against noise since RJMCMC reconstruction uses a shape constraint via the peak-by-peak approach and an explicit noise model.

6. ACKNOWLEDGEMENTS

We would like to thank Prof. Ray Freeman (Jesus College, Cambridge University) and Dr. Eriks Kupce (Varian Ltd., Oxford) for their assistance, advice, and for providing the data sets we use.

REFERENCES

[1] G. Bodenhausen and R. R. Ernst, "Direct Determination of Rate Constants of Slow Dynamic Processes by Two-Dimensional Accordion Spectroscopy in Nuclear Magnetic Resonance" *Journal of American Chemical Society*, vol. 104, pp. 1304–1309, 1982.

[2] S. Kim and T. Szyperski, "GFT NMR, a new approach to rapidly obtain precise high-dimensional NMR Spectral information" *Journal of American Chemical Society*, vol. 125, pp. 1385–1393, 2003.

[3] R. Freeman and E. Kupce, "Distant Echoes of the Accordion - Reduced Dimensionality, GFT-NMR, and Projection-Reconstruction of Multidimensional Spectra" *Concepts in Magnetic Resonance Part A*, vol. 23A, 2004.

[4] E. Kupce and R. Freeman, "Fast Multidimensional NMR Spectroscopy by the Projection-Reconstruction Technique" *Spectroscopy*, October. 2004.

[5] E. Kupce and R. Freeman, "The Radon Transform: A new Scheme for Fast Multidimensional NMR" *Concepts in Magnetic Resonance Part A*, vol. 22A, pp. 4–11, Dec. 2003.

[6] E. Kupce and R. Freeman, "Projection-Reconstruction of Three-Dimensional NMR Spectra" *Journal of Americal Chemistry Society*, vol. 125, No. 46, pp. 13958–13959, 2003.

[7] E. Kupce and R. Freeman, "Projection-Reconstruction Technique for Speeding up Multidimensional NMR Spectroscopy"

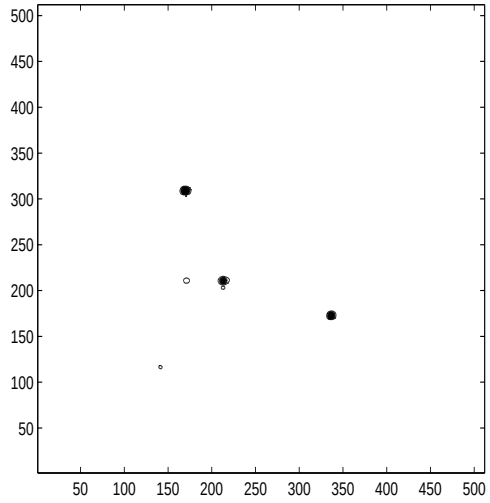

Figure 5: A contour image from Maximum Entropy

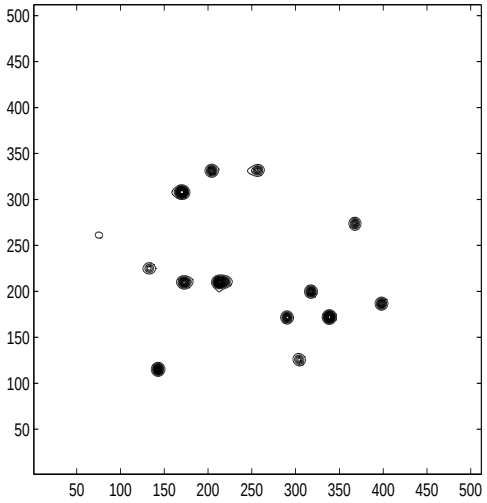

Figure 7: A contour image from RJMCMC

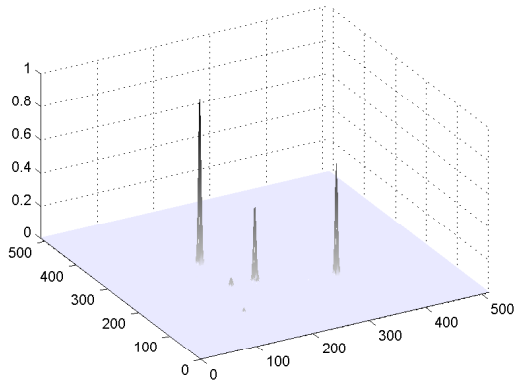

Figure 6: A mesh image from Maximum Entropy

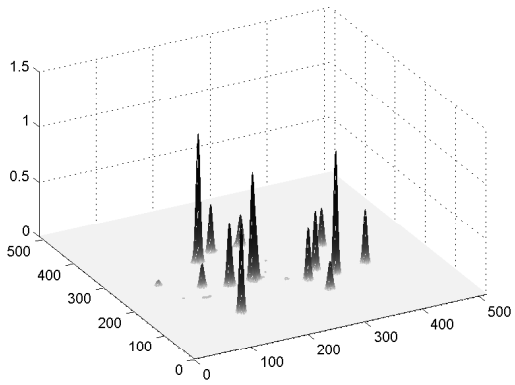

Figure 8: A mesh image from RJMCMC

Journal of American Chemical Society, vol. 126, pp. 6429–6440, Jan. 2004.

[8] G. Kontaxakis and L. G. Strauss "Maximum Likelihood Algorithms for Image Reconstruction in Positron Emission Tomography" *Radionuclides for Oncology*, pp. 73–106, 1998.

[9] A. P. Dempster and N. M. Laird and D. B. Rubin "Maximum Likelihood from incomplete data via the EM algorithm" *Journal of Royal Statistical Society*, vol. 39, pp. 1–38, 1977.

[10] A. M. Djafari "Maximum Entropy Principle and Linear Inverse Problems" *Applied Mathematics and Optimization Journal*, 1992.

[11] G. Minerbo "MENT: A maximum entropy algorithm for reconstructing a source from projection data" *Computer Graphics and Image Processing*, vol. 10, no. 1, pp. 48–68, May. 1979.

[12] M. L. Reis and N. C. Roberty "Maximum entropy algorithms for image reconstruction from projections" *IOP publishing Ltd*, vol. Inverse Problems 8, pp. 623–644, Aug. 1992.

[13] J. Qi and R. H. Huesman "Fast Approach to Evaluate MAP Reconstruction for Lesion Detection and Localization" *Lawrence Berkeley National Laboratory*, One Cyclotron Road, Berkeley, CA 94720, USA, Technical report, Feb. 2004.

[14] J. Yoon and S. J. Godsill and E. Kupce and R. Freeman "Deterministic and statistical methods for reconstructing multidimensional NMR spectra" *Magnetic Resonance in Chemistry*, vol. 44, pp. 197–209, 2006.

[15] P. J. Green, "Reversible Jump Markov Chain Monte Carlo computation and Bayesian model determination" *Biometrika*, pp. 711–732, 1995.

[16] P. J. Green, "Highly Structured Stochastic Systems" *OUP*, chapter: Trans-dimensional Markov chain Monte Carlo, 2003.

[17] G. Casella, C. P. Robert "Rao-Blackwellisation of sampling schemes" *Biometrika*, vol. 83, pp. 81–94, 1996.

[18] S. J. Godsill, "On the Relationship Between Markov Chain Monte Carlo Methods for Model Uncertainty" *Journal of Computational and Graphical Statistics*, vol. 10, pp. 1–19, 2001.

[19] J. Vermaak, C. Andrieu, A. Doucet and S. J. Godsill "Reversible Jump Markov Chain Monte Carlo strategies for bayesian model selection in autoregressive processes" *Journal of Time series analysis*, vol. 25, pp. 785–809, 2004.